

Towards Biodegradable Barrier Packaging: Production of Films for Single-Use Primary Food Liquid Packaging

Nanci Ehman,* Agustina Ponce de León, Fernando E. Felissia, and M. Cristina Area

Award Winner: 2021 BioResources Early Career Investigator Award

This research aimed to obtain bio-degradable microfibrillated cellulose (MFC) films from a pine sawdust pulp for use as liquid containers. The films were combined with food-grade polyols (sorbitol, glycerol, and mannitol) to improve the hydrophobicity and provide barrier properties. Pine sawdust (a by-product of primary wood industrialization, highly available, and inexpensive) was treated with soda-ethanol and a 2-stage oxygen sequence. The resulting pulps were mechanically fibrillated to produce MFC with a disk refiner. The polyols were added to improve crosslinking and achieve a plasticizing effect. The films were dried at 25, 50, and 60 °C. The mechanical and barrier properties (tensile strength, elongation, vapor permeability, and water absorption), the crystallinity, and the transparency of the films were evaluated. Total migration tests were carried out to verify the compliance of the films with current regulations. Finally, the film's biodegradation properties in soil under normal climatic conditions were evaluated.

DOI: 10.15376/biores.17.3.5215-5233

Keywords: Microfibrillated cellulose; MFC; Biorefinery; Pine sawdust; Plasticizers; Biodegradable films

Contact information: IMAM, UNaM, CONICET, Programa de Celulosa y Papel (PROCYP), Félix de Azara 1552, Posadas, Argentina; *Corresponding author: nanciehman@gmail.com

INTRODUCTION

One of the most pressing environmental problems is the disposal of single-use plastics. Among these plastics, one of the main contributors to contamination is food containers. The plastic materials that are currently used for food containers have good barrier properties to water, steam, oils, and fats, but they have poor biodegradation abilities (Fresán *et al.* 2019). The cycle of use is estimated in days or weeks according to the type of food they protect, while its degradation period after the food is consumed can reach up to thousands of years. Oxo-degradable materials produce micro and nanoplastics (Gorycka 2009; Peng *et al.* 2020). In most cases, the products in contact with food are contaminated with organic material, which makes their reuse or recycling difficult. These detrimental effects are contradictory for a single-use material, since its degradation would take longer than its useful life.

Food protection containers are divided into primary (direct contact with food), secondary (containing the primary packaging), and tertiary (involving one or more secondary packaging) (MERCOSUR 2002) (Fig. 1). Primary food containers involve glass, metals, paper or cardboard, and mainly plastics (rigid and flexible forms) (Marsh and

Bugusu 2007). While some newer plastics are biobased, most are made from petroleum and include additives such as polymers.

The most used material in food packaging is polyethylene (PE). Polyethylene, which is obtained from non-renewable and non-biodegradable sources, is used as packaging for products with very short life cycles (bags, containers for water and beverages, or containers for hygiene and cleaning products) (European Bioplastics 2019; Fresán *et al.* 2019).

In papers and cardboards, primary packaging usually contains a layer of PE or polypropylene (PP), which provides the required barrier property. Figure 1a shows a typical multilayer liquid container. Usually, the cardboard is formed with an unbleached paper and a bleached layer. The unbleached layer is the main contributor to the mechanical strength of the container, and the bleached layer improves the printing to make the container more visually appealing.

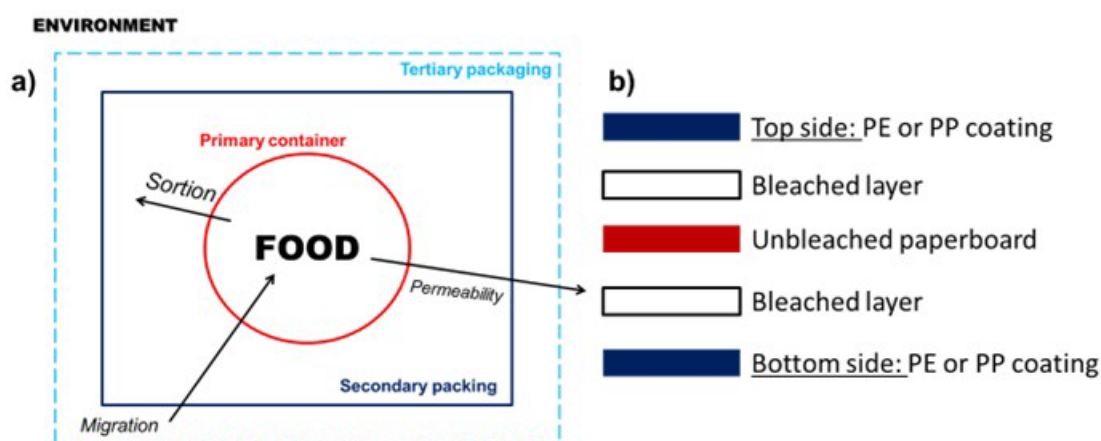


Fig. 1. The a) multilayer liquid packaging diagram and the b) food packaging classification. Adapted from (MERCOSUR 2002)

Finally, one or more coatings of PE or PP are applied to improve the hydrophobicity of the material. In all cases, coatings must meet specific properties (such as mechanical, barrier, or optical) according to their use, and they must have the least material migration on the food they contain according to current regulations (Table 1) (Ariosti 2021). The material migration is measured *via* the overall migration limit (OML).

Table 1. Regulations that Mention the Migration Limits of Materials

Regulation	Region or Country	OML (mg/kg)
Código Alimentario Argentino (CAA)	Argentina	8 mg/dm ² (cellulosic based materials)
GMC MERCOSUR Regulations	MERCOSUR countries	60 (or 10 mg/dm ²)
Food and drug administration (FDA)	USA	50 (or 0.5 mg/in ² , 7.75 mg/dm ²)
Regulation (EC) No 1935/2004	European Union and EEE countries	60 (or 10 mg/dm ²)
Guobiao (GB) Standards	China	60 (or 10 mg/dm ²)

However, PE or PP coating on the paper or cardboard reduces its reusability, recyclability, and biodegradability (Schoukens *et al.* 2014). Strategies have been evaluated to replace these single-use materials with more environmentally friendly alternatives obtained from renewable sources (for example, from other processes by-products), using an integrated process (complete approaching of raw material), and with short periods of biodegradation. Microfibrillated cellulose (MFC) obtained from pine sawdust biorefinery pulps is a promising candidate. The pine sawdust biorefinery processes involve treatments that allow the different components of the raw material to be separated to produce high-value products. The pine sawdust is generated in primary wood industries and is usually accumulated in the same place or burned in the open air.

MFC could be obtained in a typical pulp and paper mill from the mechanical fibrillation of pulps through disc refiners. Test with the addition of MFC have shown improvements in the mechanical and barrier properties of paper and cardboard (Lavoine *et al.* 2012; Merayo *et al.* 2017). However, MFC films exhibit a hydrophilic character and low flexibility. One of the possible strategies for reducing these problems is combining MFC with plasticizers (Mathew and Dufresne 2002; Mathew *et al.* 2008; Herrera *et al.* 2017). Plasticizers are low molecular weight substances added to a polymeric system to promote plasticity and flexibility (Adeodato Vieira *et al.* 2011). Polyols (sorbitol, mannitol, xylitol, and glycerol) are small molecules that are very effective in plasticizing polysaccharide-based polymers (Vieira *et al.* 2011).

This study aimed to evaluate the behavior of different loads of food-grade plasticizers in MFC films. Three plasticizers (sorbitol, glycerol, and mannitol) at three loads (15% w/w, 25% w/w, and 50% w/w) and three film drying temperatures (25, 50, and 60 °C) were evaluated. The physical-mechanical, optical, and water vapor permeability (WVP) properties, as well as the OMLs for materials in contact with food, were analyzed. Finally, a soil degradation analysis was carried out to assess whether these films can disintegrate under normal conditions after use.

EXPERIMENTAL

Materials

Pine sawdust was collected from a local sawmill. Analytical-grade sorbitol, glycerol, and mannitol reagents (Anedra, Buenos Aires, Argentina) were used to produce the films. Commercial-grade ethanol (15% v/v) and commercial-grade acetic acid (3% w/v) were used in the OML analysis.

Methods

A summarized scheme of the methodology that was followed is shown in Fig. 2. The pine sawdust was subjected to a soda/ethanol pulping process. The conditions were optimized in a previous study (Imlauer Vedoya *et al.* 2022).

Production and characterization of the MFC

An oxidative sequence with two oxygen stages was performed on the soda/ethanol pine pulp. The conditions were 100 °C, 60 min, 10% consistency, 600 kPa of oxygen pressure, and 3% sodium hydroxide (NaOH) charge on oven-dry pulp (odp). After each oxygen stage, the process yield, Kappa number, and intrinsic viscosity were determined.

The pulps obtained were passed by a simple disk refiner at 1% consistency to produce the MFC. The distance between the fixed and mobile disc was 0.001 in (0.0254 mm) and the pulp circulated through the discs for 24 min.

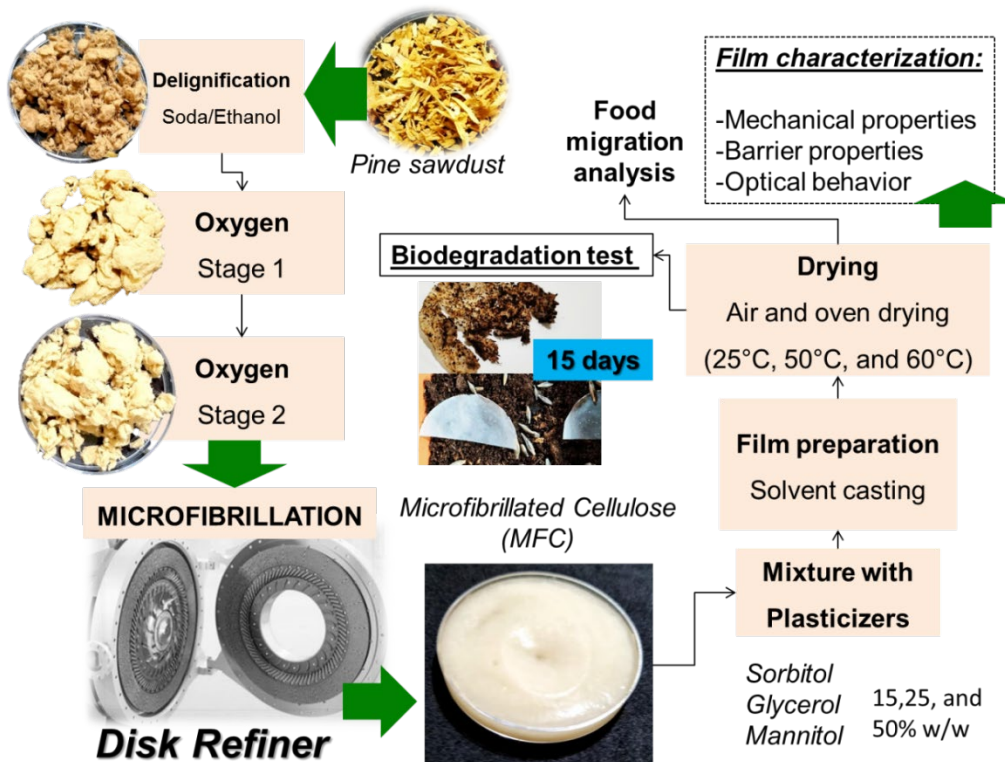


Fig. 2. The applied methodology

The MFC and pulp images were obtained using a Carl Zeiss light microscope (Zeiss, Oberkochen, Germany) combined with Leica QWin image analysis software (Leica Microsystems, Wetzlar, Germany).

MFC/plasticizer films preparation

The plasticized MFC-based films were prepared *via* solvent casting. The film mixtures included the combination of MFC and three plasticizer loads (15% w/w, 25% w/w, and 50% w/w) of sorbitol, glycerol, and mannitol. The plasticizer was placed in a beaker at room temperature and dissolved in water. Then, the MFC suspension, at 1.55% consistency, was added. The mixture at 0.5% consistency was stirred for 15 min, and the films were prepared in PP petri dishes. The samples were allowed to dry at three temperatures: 25 °C (air drying), 50 °C, and 60 °C (oven-drying). The time required for the films to dry was determined. The films without the addition of the plasticizer were used as the control.

The surface charge of MFC was measured by colorimetric titration, adapting the methodology described by Mocchiutti and Zanuttini (2007). The diluted suspension at 0.04% consistency was stirred for 30 min at 500 rpm. 15 g of sample was taken, mixed with 25 mL of 0.001N polydimethyldiallylammonium chloride (polyDADMAC), and stirred for 2 min at 500 rpm. The sample was centrifuged for 10 min at 3000 rpm. 10 mL of supernatant was taken after centrifugation, and one drop of o-toluidine blue (OTB) indicator was added. The absorbance was measured using a Shimadzu UV-1800 UV-Vis

spectrophotometer in the visible region (400-700 nm). Titration was started using potassium polyvinyl sulfate (PVSK) as the negative titrant polymer, and for each milliliter, added absorbance was measured.

The rheological properties of LCNF dispersions were measured at $25 \pm 1^\circ \text{C}$ by a Brookfield Rotational Viscometer model DV1 using a vane-type spindle at 0.6 rpm rotation speeds. 250 mL of aqueous dispersions at 0.5% consistency were prepared and then stirred for 60 min at 500 rpm to reach a homogeneous system. The torque during the measurement was kept between 10% and 50%.

After drying, the films were conditioned for 24 h at 23°C and 50% relative humidity (RH) for characterization.

Physical-mechanical properties

The film thicknesses were directly measured using a digital micrometer (Testing Machine Inc-TMI, New Castle, DE, USA) with a precision of $0.001 \mu\text{m}$. Ten measurements were carried out at random points of the four films obtained for each sample and the average value was calculated. The film grammage was determined following the TAPPI standard T410 (1998) using a digital electronic scale with 0.001 g precision.

The tensile index (TI) and elongation at break (EAB) values were measured according to the TAPPI standard T494 (1988) using a universal testing machine (Adamel Lhomargy, Roissy-en-Brie, France). The 15 mm wide specimens were tested at 50 mm between the jaws.

Optical properties

The light transmittance and the transparency were measured between 350 and 800 nm using a UV-Vis Shimadzu spectrophotometer (Kyoto, Japan). Three samples with dimensions of $10 \text{ mm} \times 40 \text{ mm}$ (at different film positions to evaluate variations in transparency) were introduced in quartz cuvettes, using air as a reference.

The optical properties were measured by a Color Touch model ISO (Technidyne, New Albany, IN, USA) colorimeter. The CIELab values were L^* (from black to white), a^* (green to red), and b^* (from blue to yellow). Finally, the total color difference (ΔE) was determined according to Eq. 1,

$$\Delta E = \sqrt{(L^* - L^*_0)^2 + (a^* - a^*_0)^2 + (b^* - b^*_0)^2} \quad (1)$$

The values of L_0 , a_0 , and b_0 were obtained from a Color Touch primary calibration standard 90 Brightness and Color.

Barrier properties

The WVP tests were carried out following the ASTM E96-00 standard (1996). Acrylic cells provided with standard 60 mm diameter holes filled with silica grit (0% RH) were used for these tests.

The devices were placed in a desiccator conditioned to a RH of 75% using saturated sodium chloride (NaCl). The water vapor pressure difference on both sides of the film provided the driving force for the water vapor flow. The weight differences in a 20 h period were used to calculate the water vapor transmission rate (WVTR). The WVP was determined by Eq. 2,

$$WVP \left(\frac{g \text{ mm}}{m^2 \text{ d kPa}} \right) = \left(\frac{WVTR}{P * RH} \right) * t \quad (2)$$

where P is the partial pressure of the water saturation vapor (Pa), RH is the relative humidity of the desiccator (%), and t is the thickness of the film (m).

The water permeability was evaluated according to TAPPI T835 (1994). The method consisted of dropping a drop of water on the film surface, and the time (in minutes) required for its complete absorption was determined (loss of sheen of the drop).

OML determination

The OML of packaging material is the total amount of components transferred from the contact material to food (MERCOSUR 2002; ANMAT 2021). Regulations allow this analysis to be carried out using food simulants (Table 2).

The test makes it possible to obtain the sum of all the compounds that migrate from the plastic material to the simulant without considering toxicological aspects, sanitary or other.

The effects of oil/fat-free liquid simulants were evaluated. The specimens, cut in duplicate, were immersed in distilled water, 3% w/v acetic acid, and 15% v/v ethanol for 24 h at 25°C. The OML was calculated according to Eq. 3,

$$OML \left(\frac{mg}{Kg} \right) = \frac{R}{A} * \frac{S}{V} \quad (3)$$

where OML is the overall migration limit (mg/kg), R is the dry weight of the residue in the simulant (mg), A is the total area of contact of the sample with the simulant (dm²), and S/V is the area/mass ratio of water corresponding to the actual contact volume between the plastic material and the food.

Table 2. The OML's for Food Simulants (Adapted from MERCOSUR 2002)

Type	Classification	Simulant	Description Simulant
I	Aqueous non-acidic foods (pH>5)	A	Distilled water (A)
II	Aqueous acidic foods (pH<5)	B	3% (m/v) acetic acid solution in distilled water (B)
III	Aqueous non-acidic foods that contain fats or oils	A and D	Distilled water and refined olive oil
IV	Fatty foods	D	Refined olive oil
V	Alcoholic foods (alcohol content >5% v/v)	C	5% (v/v) ethanol solution in distilled water or ethanol solution in distilled water
VI	Dry foods or with little extractive action significant	None or occasionally A, B, C, or D, according to the type of food	

Soil biodegradability tests

The film samples were buried in soil using pots located 2 cm from the surface (aerobic biodegradation) with fast-growing grass seeds. The pots were stored in the open air under normal climatic conditions (summer in Argentina). Weight loss is the usual physical method to assess biodegradation in samples. The films were buried in soil under normal plant growth conditions with the following methodology. First, the films were oven-dried at 80 °C for 1 h and then weighed. They were then planted with common grass in the open air and analyzed after 15 d. All the samples showed evidence of biodegradation.

After 15 d, the films were reweighed, and the percentage of biodegradation was calculated using Eq. 4,

$$\text{Biodegradation (\%)} = \left(\frac{W_{15} - W_0}{W_0} \right) * 100 \quad (4)$$

where W_0 is the initial weight film (g) and W_{15} is the film weight after the 15 d burial period (g).

X-ray diffraction (XRD)

The XRD patterns of the films were analyzed using an X-ray diffractometer (Rigaku SmartLab SE X-ray, Japan) with a monochromatic source $\text{CuK}\alpha 1$ over an angular range of 10° to 60° . (Rigaku SmartLab SE X-ray, Japan)

Statistical analysis

Statgraphics software (Statgraphics Technologies, The Plains, VA, USA) was used for statistical analyses at a 95% confidence level.

RESULTS AND DISCUSSION

The yields, Kappa number, and intrinsic viscosity for the different stages are shown in Table 3.

Table 3. Properties of the Pulp after each Oxygen Stage

Stage	Yield (%)	Kappa Number	Intrinsic Viscosity (mL/g)
Oxygen 1	96.9	11.0 ± 0.00	446 ± 3.26
Oxygen 2	96.1	6.80 ± 0.00	400 ± 2.40

The use of oxygen delignification sequences has numerous benefits over chlorine or its derivatives. Oxygen delignification contributes lower loads to the effluents and reduces the cost of operation concerning chlorine or its derivatives. The intrinsic viscosity between the stages did not vary significantly, showing the sequence selectivity (Fig 3a).

The lignin removal in kraft hardwood pulp when O-O is used is between 35% to 50%, while the lignin removal in softwood pulps can reach as high as 65% (Sixta 2006). The high percentage of delignification is carried out without affecting the oxygen selectivity or the physical properties of the pulps obtained (Sixta 2006). The proposed sequence applied on soda/ethanol pine sawdust pulp allowed 60.6% delignification. The intrinsic viscosity between the stages did not vary significantly, which shows the sequence selectivity (Fig 3a).

The MFC characterization is shown in Table 4. The process of obtaining MFC does not involve losses of material. The yield loss was due to pulp remaining between the disc refiner and other equipment parts, which made the fibers difficult to extract.

Table 4. MFC Characterization

Yield Process (%)	Surface Charge ($\mu\text{eqg/g}$)	Intrinsic Viscosity (mL/g)	Dynamic Viscosity in Water (Pa.s)	CI (%)
77.0	270 ± 9.23	343 ± 5.41	105 ± 0.194	74.3

The interaction of polyDADMAC with MFC involves factors such as adsorption of the polymer on the MFC and the interaction on surface with the carboxylic groups by ionic-exchange mechanism (Espinosa *et al.* 2015). The cationic polymer fixation by the surface unit of cellulose for a mechanical treatment reaches a constant value for a level of fibrillation. So, the high values in the surface density of negative charges become negligible, and the adsorption of the polymer by Van der Waals interactions and the hydrogen bonding are considerable (Rouger and Mutje 1984). Therefore, the value in the charge density of the MFC sample indicates a greater surface area in the sample, showing the greater fibrillation in the sample. The results obtained for MFC suspension are lower than those of a bleached eucalyptus kraft pulp treated with a sequence PFI-homogenizer (Delgado Aguilar 2015) and similar to those of triticale pulp only treated with a homogenizer (Tarrés *et al.* 2017).

The MFC suspensions obtained had a gel-like aspect. The gel-like aspect is explained by a matrix structure formation due to the high aspect ratio of the microfibers and the charged surface that produce H bonds between the fibrils and electrostatic repulsion between the samples. The factors that influence the rheology properties in MFC suspensions can be divided into the morphology aspects (sizes, shapes) and surface chemical composition. The morphology aspect depends on the raw material (particularly length and width of the fiber) but mainly on the fibrillation process and network structure, whilst the surface chemistry includes the influence of the functional groups on the surface (Hubbe 2017).

Figure 3b shows the MFC suspension obtained using the disc refiner. The MFC process yield was 77.0%. The yield loss was due to pulp remaining between the disc refiner and other equipment parts, which made the fibers difficult to extract.

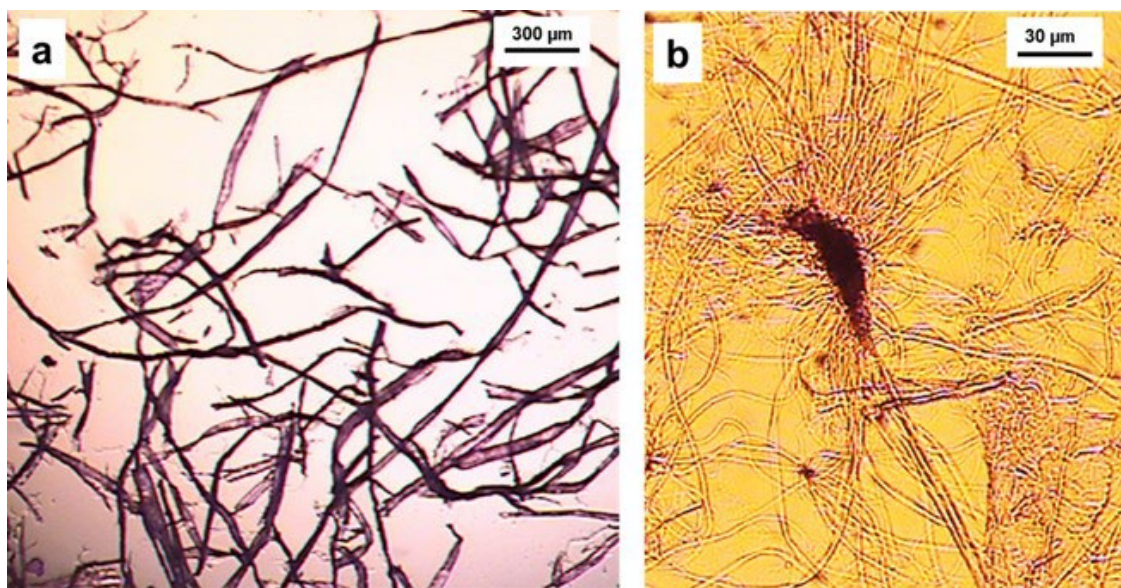


Fig. 3. The microscopic images of the a) soda-O-O pulp and the b) MFC suspension

The microscopic images showed a highly microfibrillated suspension with some residual fibers. Fibers with almost complete microfibrillation were also observed.

Physical-mechanical properties for films

The required drying time for the films was 120 h for samples dried at 25 °C, 48 h at 50 °C, and 24 h at 60 °C. The grammage values ranged between 20 and 30 g/m². These values are similar to PE coatings found on the market. Containers for liquids are usually made of multilayer cardboard with one or more outer and inner layers of PE or PP. These coatings have grammages from 12 to 30 g/m² (Stora Enso 2021).

The films thickness average ranged from 26.9 to 71.6 µm. The thickness values were similar to those obtained when carboxymethyl cellulose, gelatin, and chitosan are combined with sorbitol and glycerol (Bakry *et al.* 2017). The addition of the plasticizer significantly increased the thickness ($p < 0.05$), which can be explained by the higher solids content for the formed film (Han and Krochta 1999). This also explains why the plasticizer load increased the film thickness values ($p < 0.05$), maximizing loads of 50% w/w. No significant differences were found for the type of plasticizer factor. However, compared to glycerol, the analysis showed a trend towards higher thickness for sorbitol films. The differences between smaller thicknesses of glycerol concerning sorbitol can be attributed to the variations in its molar mass. This behavior was previously observed when sorbitol and glycerol were applied to starch films (Sanyang *et al.* 2016).

The application of plasticizers in films reduced the TI values ($p < 0.05$), which could be a contradictory effect. However, it makes sense due to the morphology of the MFC (Table 4). Usually, MFCs are applied to increase the tensile indexes due to their elongated morphology, which allows a more woven structure. The MFC load is reduced when a plasticizer is added. This reduces the mechanical reinforcement, a behavior observed in previous MFC and polyols antibacterial films (Liu *et al.* 2013; Aliabadi *et al.* 2021). Opposite results (an increase in the TI) were obtained for cellulose nanocrystals (CNC) with the addition of mannitol, sorbitol, and glycerol. However, this finding was related to the morphology of the CNC (short structures that produce a fragile and brittle film) (Fernández-Santos *et al.* 2021). The decreases in the TI, compared with the control sample (73.3 N m/g), were higher as the plasticizer load increased ($p < 0.05$). This was also seen when CNC samples are combined with sorbitol and glycerol (Talja *et al.* 2007).

The analysis of variance (ANOVA) analysis showed significant differences between the samples dried in the air or the oven ($p < 0.05$). However, the samples that were dried at 50 and 60 °C did not show significant differences (Table 5). The lower TI values of the air-dried samples may be due to the crystallization of plasticizers when drying in the presence of high humidity. If this type of crystallization occurs, a film with white spots is observed (Talja *et al.* 2007). Photos are shown in the next section.

Table 5. The TI and EAB Values

Sample	TI (N m/g)			EAB (%)		
	25 °C	50 °C	60 °C	25 °C	50 °C	60 °C
CONTROL	73.4 ± 7.55	86.9 ± 3.70	57.6 ± 8.01	5.02 ± 0.98	6.46 ± 0.52	3.59 ± 0.41
SOR-15	52.6 ± 7.86	52.6 ± 4.65	56.9 ± 3.85	5.52 ± 0.71	8.52 ± 0.72	7.28 ± 0.67
SOR-25	16.9 ± 0.15	34.5 ± 6.66	34.6 ± 3.08	9.97 ± 1.09	7.77 ± 0.41	8.06 ± 0.71
SOR-50	11.0 ± 1.57	25.3 ± 5.55	13.4 ± 2.66	8.94 ± 0.86	12.4 ± 1.10	8.79 ± 0.34
GLY-15	38.8 ± 4.97	56.2 ± 8.94	54.5 ± 3.28	6.09 ± 0.55	7.82 ± 0.54	7.36 ± 0.69
GLY-25	21.9 ± 4.54	62.8 ± 3.73	47.0 ± 7.20	11.5 ± 0.25	8.51 ± 0.28	7.85 ± 0.83
GLY-50	2.7 ± 0.65	15.4 ± 3.02	17.4 ± 1.56	8.58 ± 0.43	7.21 ± 0.73	6.49 ± 0.16
MAN-15	69.2 ± 3.10	54.7 ± 9.70	66.5 ± 6.10	4.82 ± 0.48	3.78 ± 0.17	5.34 ± 0.23
MAN-25	50.5 ± 3.28	46.6 ± 5.01	43.3 ± 4.76	5.08 ± 0.20	5.15 ± 0.50	2.79 ± 0.16
MAN-50	3.9 ± 0.18	47.2 ± 3.17	61.8 ± 6.58	1.17 ± 0.15	1.67 ± 0.03	1.34 ± 0.03

The application of plasticizers significantly modified the EAB properties ($p < 0.05$). Improved EAB values were observed for the MFC samples mixed with sorbitol and glycerol (Table 4). However, for those samples where mannitol was applied, the EAB values decreased by up to 76.7% (50% w/w mannitol, dried at 25 °C). This brittle behavior is similar to that seen when mannitol and CNC are combined (Fernández-Santos *et al.* 2021). The highest elongation changes occurred at a drying temperature of 60 °C ($p < 0.05$), but no significant differences were obtained at temperatures of 25 °C and 50 °C.

The plasticizer load was a significant factor ($p < 0.05$), with the highest changes observed with 25% w/w of plasticizer. The elongation results were similar to those found in other studies where polyols with CNC were applied (Talja *et al.* 2007; Csiszár and Nagy 2017; Fernández-Santos *et al.* 2021).

Visual appearance and optical behavior

The appearance of the films was variable (Fig. 4a). The combinations between the MFC and sorbitol had a similar appearance to the control. However, the glycerol and mannitol samples showed different appearances. In the case of the sample that contained glycerol, the films mostly stuck to the petri dishes, which made their removal difficult. The films were sticky and ripped easily, and this behavior increased with the glycerol loading. This behavior coincides with the results of Sanyang *et al.* (2016).

The mannitol films were very brittle, and typical white spots of the polyol crystallization were observed in the framework (Fig. 4b). This staining effect was more frequent in air-dried mannitol samples.

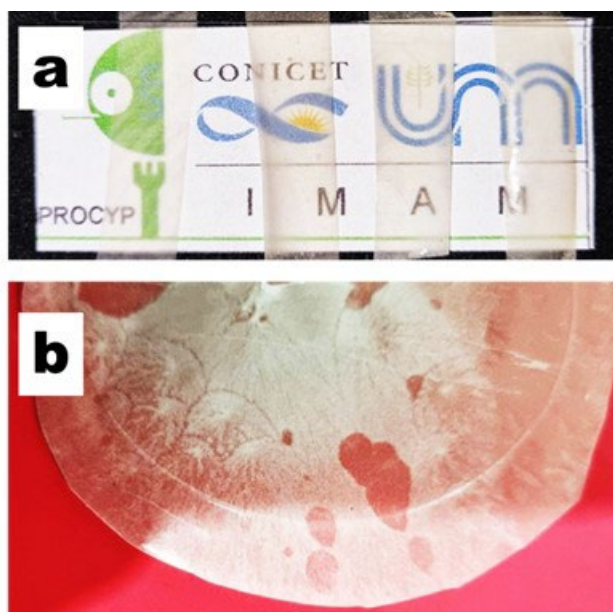


Fig. 4. a) Samples dried at 50 °C. From left to right: control, 25%w/w sorbitol, 25% w/w glycerol, and 25% w/w mannitol. b) Films obtained using 50% w/w mannitol dried at 25 °C

The increase in the plasticizer load produced increases in the transmittance values at 600 nm ($p < 0.05$). The highest transmittance values were obtained for the samples that contained a 50% w/w plasticizer load, while the 15% w/w plasticizer load produced the lowest transmittance values. The type of plasticizer also influenced the films transmittance ($p < 0.05$). Other authors also observed increases in transmittance when glycerol and

sorbitol were applied as plasticizers (Bakry *et al.* 2017). For samples with mannitol, the areas free of stains were chosen for the transmittance analysis at 600 nm. Mannitol maximized the transmittance values at 600 nm (up to 18.1% transmittance), while the use of glycerol produced lower values than the control (3.51% transmittance). Figure 5 shows the transmittance spectrum for wavelengths between 350 and 800 nm (films dried at 25 °C). The drying temperature did not influence the transmittance values.

The total color difference estimates the visual appearance of the product and the acceptance for consumers (Ballesteros-Mártinez *et al.* 2020). They ranged between 14.3 and 17.1. The incorporation of plasticizers did not produce statistically significant changes in the total color difference. The same behavior was observed for the drying temperature and the incremental loads of mannitol, sorbitol, or glycerol.

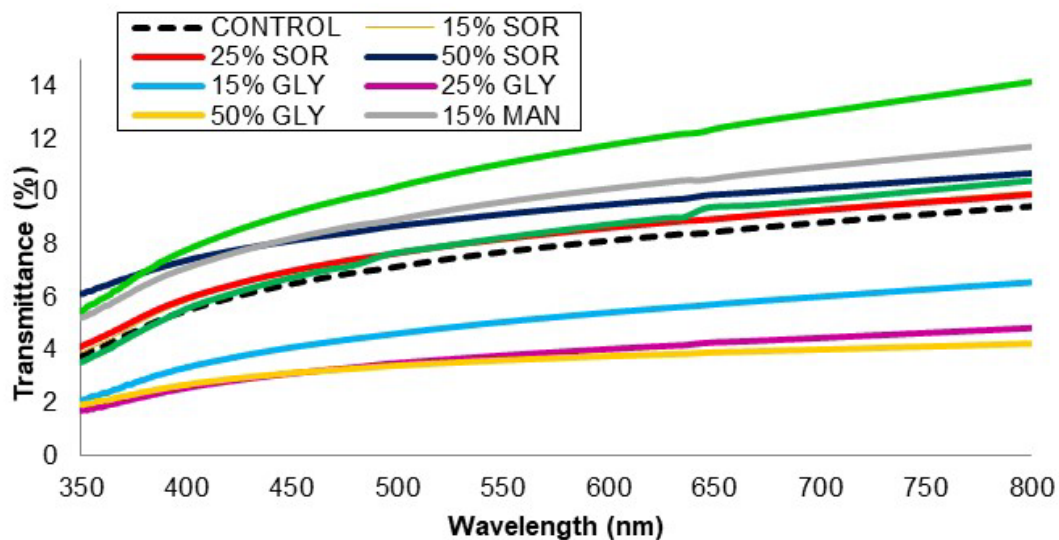


Fig. 5. Transmittance spectrum for the samples dried at 25 °C

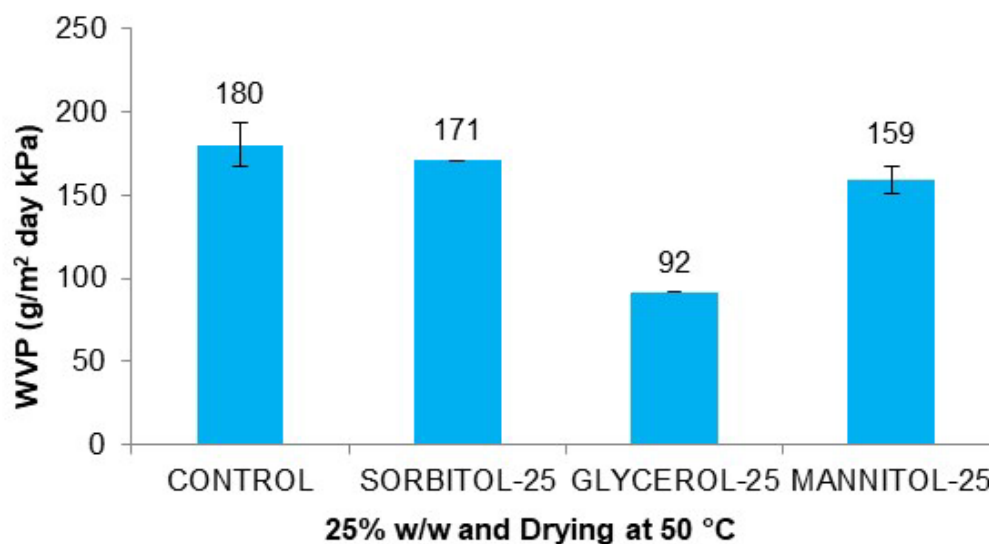


Fig. 6. WVP values at 25% w/w load and 50 °C of drying

Barrier properties

The WVP is relevant to the shelf life of the food contained by the film. A high permeability will cause greater diffusion of water within the product, accelerating its deterioration. The addition of the plasticizers had a significant effect on the WVP values ($p < 0.05$), which decreased in all cases compared with the control samples (Fig. 6). No significant differences were observed for variable loads or drying temperatures. The values were similar to those obtained when CNC was combined with sorbitol and glycerol (Fernández-Santos *et al.* 2021) and when citric acid and glycerol were applied in starch film (Herrera *et al.* 2017). In food applications, films with good water insolubility are required to provide water resistance and increase the shelf life of the contained food products (Sanyang *et al.* 2016).

The values in the film water absorption when using the water drop test (WDT) were similar to those obtained when CNC was combined with polyols such as sorbitol, glycerol, and mannitol (Fernández-Santos *et al.* 2021). However, the addition of plasticizers increased the water absorption of the samples over the control. This effect was found by other authors and is due to the hydrophilic nature of the applied polyols since they weaken the cellulose interactions by increasing the free spaces between chains (Müller *et al.* 2008; Maran *et al.* 2013; Chiumarelli and Hubinger 2014). The ANOVA analysis for the water permeability variable showed that the addition of polyols reduced the absorption time of the water drop by 59.4% ($p < 0.05$). The films with plasticizers took 30 to 60 min to achieve total water absorption.

A possible solution to reduce the hydrophilic character of the films could be the reduction of the OH groups in the MFC by chemical modifications. Acetylation is one of the most studied methods for reducing fibers' moisture absorption, and studies were extrapolated to nanocellulose (Ávila Ramirez *et al.* 2014). The modification consists of the OH groups replacement with acetyl groups through esterification reactions using acetic acid or acetic anhydride, and in some cases, acid catalysts are incorporated (Herrera *et al.* 2017). Other modifications to increase the hydrophobicity of the films could involve grafting (Lakovaara *et al.* 2021), reaction with silane groups, or surfactants (Abdul Khalil *et al.* 2012; Islam *et al.* 2013). The combination of nanocellulose and thermoplastics is another interesting option (Hakimi *et al.* 2021). However, the studies generally involve thermoplastic as matrix and cellulosic derivatives as reinforcement (Ruz-Cruz *et al.* 2022).

OML of the films

The ANOVA analysis showed significant differences between the factors added plasticizer ($p < 0.05$), plasticizer load ($p < 0.05$), and type of simulat ($p < 0.05$). In the case of the drying temperature, no significant differences were observed between the samples. However, the trend shows that the values at 60 °C were lower (Table 6).

Table 6. OML Values for Simulants A, B, and C

Sample	OML (mg/kg)								
	25 °C			50 °C			60 °C		
	A	B	C	A	B	C	A	B	C
CONTROL	0.00	15.8	33.3	0.00	19.0	19.0	0.00	22.2	25.0
SOR-15	16.2	85.5	71.4	40.0	57.0	59.2	61.5	50.7	48.8
SOR-25	70.0	177	92.9	71.2	185	125	66.2	168	105
SOR-50	104	421	113	230	262	174	242	220	175
GLY-15	35.0	38.0	29.8	27.5	47.5	23.8	11.2	23.8	30.9
GLY-25	77.5	85.0	23.8	60.0	90.0	55.9	61.2	82.4	35.7
GLY-50	211	213	321	182	298	249	102	128	102
MAN-15	55.0	69.7	75.0	35.0	47.5	123	36.2	104.6	47.6
MAN-25	57.5	228	94.8	354	241	252	80.0	82.0	123
MAN-50	197	247	250	63.7	124	72.6	310	342	180

The simulant with the highest OML was 15% v/v ethanol, while no differences were observed between simulants A and C. The increase in the plasticizer load increased the total migration values. Those films with 15% w/w of plasticizer were within the acceptable OML limits (except for the mannitol in simulants B and C). Finally, the lowest increases in the OML values were observed for the samples with glycerol.

Biodegradation tests

Figure 7a shows the samples planted with grass seeds (bottom) and the biodegraded samples (top).

The films combined with glycerol and sorbitol disappeared from the pots, reaching 100% biodegradation. The increase in film biodegradation with sorbitol addition was demonstrated in starch samples combined with sorbitol and chitosan (Arief *et al.* 2021).

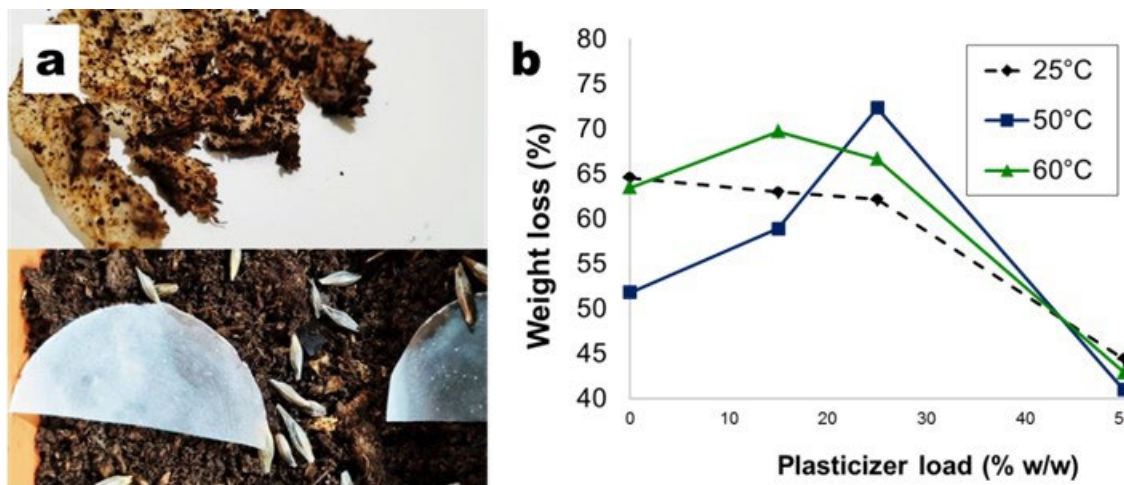


Fig. 7. a) Films before (bottom) and after (top) 15 d buried in soil; b) weight loss for the mannitol samples

Similarly, the increase in glycerol loading allowed a biodegradation increase in cassava starch films (Theamdee and Pansaeng 2019). The –OH and –COOH functional groups that possess flexible active sites can degrade at high rates, as these groups allow the film to bind to enzyme sites faster. In addition, polymers with shorter chains are known to degrade faster than complex chemical structure polymers (which require additional

enzymes). Opposite to the glycerol and sorbitol, the control samples and the films where mannitol was added did not complete their biodegradation in that period (Fig. 7b).

The effect of the lower biodegradation of mannitol concerning the other two polyols may be due to its crystalline structure, which can be verified in the spectra obtained by XRD. The samples with glycerol and sorbitol decreased the intensities of the crystalline peaks as the load increases (Fig. 8a).

This behavior was not present in mannitol samples (Fig. 8b). The effect of the crystalline structure on biodegradation has been previously demonstrated (Li *et al.* 2015). Amorphous zones are points where degradative enzymes can enter and cause biodegradation. Li *et al.* (2015) also found that the presence of simple molecular structures allows the samples to biodegrade in a lower period.

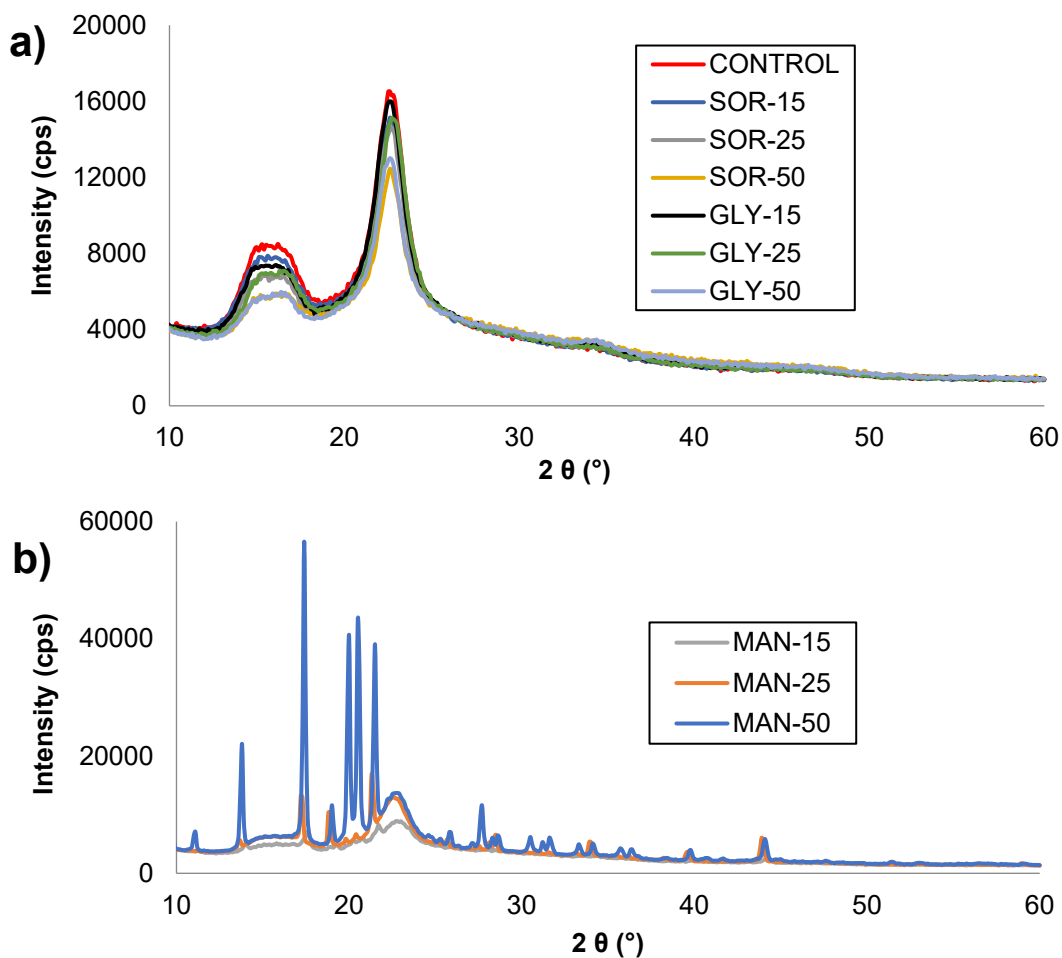


Fig. 8. XRD spectrum of the a) control, sorbitol, glycerol samples and the b) mannitol samples dried at 50 °C

CONCLUSIONS

1. It is possible to obtain microfibrillated cellulose (MFC) films from pine sawdust combined with sorbitol, glycerol, and mannitol as plasticizers with improved water vaper permeability (WVP) reduction and elongation at break (EAB) properties. The biodegradability of the films also improved with the addition of the sorbitol and glycerol.
2. The addition of plasticizers did not increase other properties such as the water absorption, transparency, and tensile strength.
3. The implementation of plasticizers at high loads produces overall migration limits (OMLs) higher than those allowed according to current regulations.
4. The addition of glycerol and sorbitol to the films achieved complete biodegradation in 15 d. However, this effect was not observed with the mannitol-containing films.

ACKNOWLEDGMENTS

The authors would like to acknowledge the financial support of the National Scientific and Technical Research Council (CONICET, Argentina) and the National University of Misiones (Argentina).

AWARD ANNOUNCEMENT

This article was submitted by Dr. Nanci Ehman to *BioResources* as part of the submission competition for the 2021 *BioResources* Early Career Investigator Award. Dr. Ehman's work was selected as the winner for the award. Congratulations to Dr. Ehman and her team!



REFERENCES CITED

- Abdul Khalil, H. P. S., Bhat, A. H., and Ireana Yustra, A. F. (2012). "Green composites from sustainable cellulose nanofibrils: A review," *Carbohydrate Polymers* 87, 963-979. DOI: 10.1016/j.carbpol.2011.08.078
- Adeodato Vieira, M. G., Altenhofen da Silva, M., Oliveira dos Santos, L., and Masumi Beppu, M. (2011). "Natural-based plasticizers and biopolymer films: A review," *European Polymer Journal* 47(3), 254-263. DOI: 10.1016/j.eurpolymj.2010.12.011.
- Aliabadi, M., Chee, B. S., Matos, M., Cortese, Y. J., Nugent, M. J. D., de Lima, T. A. M., Magalhães, W. L. E., de Lima, G. G., and Firouzabadi, M. D. (2021). "Microfibrillated cellulose films containing chitosan and tannic acid for wound healing applications," *Journal of Materials Science: Materials in Medicine* 32(6), 67. DOI: 10.1007/s10856-021-06536-4
- ANMAT. (2021). "Capítulo IV: Utensilios, recipientes, envases, envolturas, aparatos y accesorios [Chapter IV: Utensils, containers, casings, appliances and accessories]," in: *Código Alimentario Argentino [Argentine Food Code]*, pp. 1-290.
- Arief, M. D., Mubarak, A. S., and Pujiastuti, D. Y. (2021). "The concentration of sorbitol on bioplastic cellulose based carrageenan waste on biodegradability and mechanical properties bioplastic," *IOP Conference Series: Earth and Environmental Science* 679. DOI: 10.1088/1755-1315/679/1/012013
- Ariosti, A. (2021). "Seminario aptitud sanitaria de envases alimentarios [Sanitary aptitude seminar for food packaging]," in: *Instituto Argentino del envase [Argentine Institute of Packaging]*, pp. 1-41.
- ASTM E96-00 (1996). "Standard test methods for water vapor transmission of materials," ASTM International, West Conshohocken, PA, USA.
- Ávila Ramírez, J. A., Suriano, C. J., Cerrutti P., and Foresti, M. L. (2014). "Surface esterification of cellulose nanofibers by a simple organocatalytic methodology," *Carbohydrate Polymers* 114, 416-423. DOI: 10.1016/j.carbpol.2014.08.020
- Bakry, N. F., Isa, M. I. N., and Sarbon, N. M. (2017). "Effect of sorbitol at different concentrations on the functional properties of gelatin/carboxymethyl cellulose (CMC)/chitosan composite films," *International Food Research Journal* 24(4), 1753-1762.
- Ballesteros-Mártinez, L., Pérez-Cervera, C., and Andrade-Pizarro, R. (2020). "Effect of glycerol and sorbitol concentrations on mechanical, optical, and barrier properties of sweet potato starch film," *NFS Journal* 20, 1-9. DOI: 10.1016/j.nfs.2020.06.002
- Chiumarelli, M., and Hubinger, M. D. (2014). "Evaluation of edible films and coatings formulated with cassava starch, glycerol, carnauba wax and stearic acid," *Food Hydrocolloids* 38, 20-27. DOI: 10.1016/j.foodhyd.2013.11.013
- Csiszár, E., and Nagy, S. (2017). "A comparative study on cellulose nanocrystals extracted from bleached cotton and flax and used for casting films with glycerol and sorbitol plasticisers," *Carbohydrate Polymers* 174, 740-749. DOI: 10.1016/j.carbpol.2017.06.103
- Delgado Aguilar, M. (2015). *Nanotecnología en el Sector Papelero: Mejoras en Calidad y Permanencia de las Fibras de Alto Rendimiento y Secundarias en Una Economía Circular Mediante el uso de Nanofibras y el Refino Enzimático*, Ph.D. Dissertation, Girona, Spain.
- Espinosa, E., Tarrés, Q., Delgado-Aguilar, M., Gonzáles, I., Mutjé, P., and Rodríguez, A. (2015). "Suitability of wheat straw semichemical pulp for the fabrication of

- lignocellulosic nanofibres and their application to papermaking slurries,” *Cellulose* 23, 837-852. DOI:10.1007/s10570-015-0807-8
- European Bioplastics (2019). *Bioplastics Market Development Update 2019*, European Bioplastics, Berlin, Germany.
- Fernández-Santos, J., Valls, C., Cusola, O., and Roncero, M. B. (2021). “Mejora de las propiedades de films de nanocelulosa mediante la adición de plastificantes para su aplicación en la industria del embalaje de alimentos [Improvement of the properties of nanocellulose films by adding plasticizers for their application in the food packaging industry],” *Recerca i Tecnologia en Enginyeria Gràfica i Disseny a la UPC [Research and Technology in Graphic Engineering and Design at the UPC]* 2, 115-129.
- Fresán, U., Errendal, S., Craig, W. J., and Sabaté, J. (2019). “Does the size matter? A comparative analysis of the environmental impact of several packaged foods,” *Science of the Total Environment* 687, 369-379. DOI: 10.1016/j.scitotenv.2019.06.109
- Gorycka, M. (2009). *Environmental Risk of Microplastics*, Research Project, Vrije Universiteit, Amsterdam, Netherlands.
- Hakimi, N. M. F., Lee, S. H., Lum, W. C., Mohamad, S. F., Osman Al Edrus, S. S., Park, B. D., and Azmi, A. (2021). “Surface modified nanocellulose and its reinforcement in natural rubber matrix nanocomposites: A review,” *Polymers* 13, article no. 3241. DOI: 10.3390/polym13193241
- Han, J. H., and Krochta, J. M. (1999). “Wetting properties and water vapor permeability of whey-protein-coated paper,” *American Society of Agricultural and Biological Engineers* 42(5), 1375-1382. DOI: 10.13031/2013.13300
- Herrera, M. A., Mathew, A. P., and Oksman, K. (2017). “Barrier and mechanical properties of plasticized and cross-linked nanocellulose coatings for paper packaging applications,” *Cellulose* 24(9), 3969-3980. DOI: 10.1007/s10570-017-1405-8
- Hubbe, M. A. (2017). “Rheology of nanocellulose-rich aqueous suspensions: A review,” *BioResources* 12(4), 9556-9661. DOI: 10.15376/biores.12.4.Hubbe
- Imlauer Vedoya, C., Area, M. C., Raffaeli, N., and Felissia, F. E. (2021). *Study on Soda/Ethanol Delignification of Pine Sawdust for a Biorefinery* (Internal Report), PROCYP, IMAM, UNaM-CONICET, Misiones, Argentina.
- Imlauer Vedoya, C., Area, M. C., Raffaeli, N., and Felissia, F. E. (2022). “Study on soda/ethanol delignification of pine sawdust for a biorefinery,” *Sustainability* 14(11), article no. 6600 (1-14). DOI: 10.3390/su14116660
- Islam, M. T., Alam, M. M., and Zoccola, M. (2013). “Review on modification of nanocellulose for application in composites,” *International Journal of Innovative Research in Science, Engineering and Technology* 2(10), 5444-5451.
- Lakovaara, M., Sirviö, J. A., Ismail, M. Y. Liimatainen, H., and Sliz, R. (2021). “Hydrophobic modification of nanocellulose and all-cellulose composite films using deep eutectic solvent as a reaction medium,” *Cellulose* 28, 5433-5447. DOI:10.1007/s10570-021-03863-1
- Lavoine, N., Desloges, I., Dufresne, A., and Bras, J. (2012). “Microfibrillated cellulose - Its barrier properties and applications in cellulosic materials: A review,” *Carbohydrate Polymers* 90(2), 735-764. DOI: 10.1016/j.carbpol.2012.05.026
- Li, M., Witt, T., Xie, F., Warren, F. J., Halley, P. J., and Gilbert, R. G. (2015). “Biodegradation of starch films: The roles of molecular and crystalline structure,” *Carbohydrate Polymers* 122, 115-122. DOI: 10.1016/j.carbpol.2015.01.011

- Liu, K., Lin, X., Chen, L., Huang, L., Cao, S., and Wang, H. (2013). "Preparation of microfibrillated cellulose/chitosan-benzalkonium chloride biocomposite for enhancing antibacterium and strength of sodium alginate films," *Journal of Agricultural and Food Chemistry* 61(26), 6562-6567. DOI: 10.1021/jf4010065
- Maran, J. P., Sivakumar, V., Sridhar, R., and Thirugnanasambandham, K. (2013). "Development of model for barrier and optical properties of tapioca starch based edible films," *Carbohydrate Polymers* 92(2), 1335-1347. DOI: 10.1016/j.carbpol.2012.09.069
- Marsh, K., and Bugusu, B. (2007). "Food packaging - Roles, materials, and environmental issues," *Journal of Food Science* 72(3), 39-55. DOI: 10.1111/j.1750-3841.2007.00301.x
- Mathew, A. P., and Dufresne, A. (2002). "Morphological investigation of nanocomposites from sorbitol plasticized starch and tunicin whiskers," *Biomacromolecules* 3(3), 609-617. DOI: 10.1021/bm0101769
- Mathew, A. P., Thielemans, W., and Dufresne, A. (2008). "Mechanical properties of nanocomposites from sorbitol plasticized starch and tunicin whiskers," *Journal of Applied Polymer Science* 109(6), 4065-4074. DOI: 10.1002/app.28623
- Merayo, N., Balea, A., de la Fuente, E., Blanco, Á., and Negro, C. (2017). "Synergies between cellulose nanofibers and retention additives to improve recycled paper properties and the drainage process," *Cellulose* 24(7), 2987-3000. DOI: 10.1007/s10570-017-1302-1
- MERCOSUR Repeals GMC Res. No. 21/02 (2002). "Reglamento Técnico del MERCOSUR para rotulación de alimentos envasados [MERCOSUR technical regulation for packaged food labeling], MERCOSUR, Montevideo, Uruguay.
- Mocchiutti, P., and Zanuttini, M. (2007). "Key considerations in the determination of Polyelectrolyte concentration by the colloidal: Titration method," *BioResources* 2(3), 399-407.
- Müller, C. M. O., Yamashita, F., and Laurindo, J. B. (2008). "Evaluation of the effects of glycerol and sorbitol concentration and water activity on the water barrier properties of cassava starch films through a solubility approach," *Carbohydrate Polymers* 72(1), 82-87. DOI: 10.1016/j.carbpol.2007.07.026
- Peng, L., Fu, D., Qi, H., Lan, C. Q., Yu, H., and Ge, C. (2020). "Micro- and nano-plastics in marine environment: Source, distribution and threats – A review," *Science of the Total Environment* 698, 134254. DOI: 10.1016/j.scitotenv.2019.134254
- Rouger, J., and Mutjé, P. (1984). "Correlation between the cellulose fibres beating and fixation of a soluble cationic polymer," *British Polymer Journal* 16(2), 83-86. DOI:10.1002/pi.4980160207
- Ruz-Cruz, M. A., Herrera-Franco, P. J., Flores-Johnson, E. A., Moreno-Chulim, M. V., Galera-Manzano, L. M., and Valadez-González, A. (2022). "Thermal and mechanical properties of PLA-based multiscale cellulosic biocomposites," *Journal of Materials Research and Technology* 18, 485-495. DOI: 10.1016/j.jmrt.2022.02.072.
- Sanyang, M. L., Sapuan, S. M., Jawaid, M., Ishak, M. R., and Sahari, J. (2016). "Effect of plasticizer type and concentration on physical properties of biodegradable films based on sugar palm (*Arenga pinnata*) starch for food packaging," *Journal of Food Science and Technology* 53(1), 326-336. DOI: 10.1007/s13197-015-2009-7
- Schoukens, G., Breen, C., Baschetti, M. G., Elegir, G., Vähä-Nissi, M., Liu, Q., Tiekstra, S., and Simon, P. (2014). "Complex packaging structures based on wood derived products: Actual and future possibilities for 1-way food packages," *Journal of*

- Materials Science Research* 3(4), 58-67. DOI: 10.5539/jmsr.v3n4p58
- Sixta, H. (2006). *Handbook of Pulp Volume I*, Wiley-VCH, Weinheim, Germany.
- Stora Enso (2021). "Paperboard materials," (<https://www.storaenso.com/en/products/paperboard-materials>), Accessed 10 January 2022.
- Talja, R. A., Helén, H., Roos, Y. H., and Jouppila, K. (2007). "Effect of various polyols and polyol contents on physical and mechanical properties of potato starch-based films," *Carbohydrate Polymers* 67(3), 288-295. DOI: 10.1016/j.carbpol.2006.05.019
- TAPPI T410 om-98 (1998). "Grammage of paper and paperboard (weight per unit area)," TAPPI Press, Atlanta, GA.
- TAPPI T 494 om-98. (1998). "Tensile properties of paper and paperboard (using constant rate of elongation apparatus)," TAPPI Press, Atlanta, GA.
- TAPPI T835 (1994). "Water absorption of corrugating medium: Water drop absorption test," TAPPI Press, Atlanta, GA.
- Tarrés, Q., Ehman, N., Vallejos, M., Area, M. C., Delgado-Aguilar, M., and Mutjé, P. (2017). "Lignocellulosic nanofibers from triticale straw: The influence of hemicelluloses and lignin in their production and properties," *Carbohydrate Polymers* 163, 20-27. DOI:10.1016/j.carbpol.2017.01.017
- Theamdee, P., and Pansaeng, N. (2019). "The effect of glycerol on the properties of biodegradable cassava starch (saai dieow cultivar) films for plastic plant bag application," *Naresuan University Journal: Science and Technology (NUJST)* 27(4), 27-38.
- Vieira, M. G. A., da Silva, M. A., dos Santos, L. O., and Beppu, M. M. (2011). "Natural-based plasticizers and biopolymer films: A review," *European Polymer Journal* 47(3), 254-263. DOI: 10.1016/j.eurpolymj.2010.12.011

Article submitted: January 14, 2022; Peer review completed: February 5, 2022; Revised version received and accepted: June 13, 2022; Published: July 21, 2022.

DOI: 10.15376/biores.17.3.5215-5233